Constraints on Particles and Fields from Full Stokes Observations of AGN

Daniel C. Homan [1,*]**, Talvikki Hovatta** [2]**, Yuri Y. Kovalev** [3,4,5]**, Matthew L. Lister** [6]**,**
Alexander B. Pushkarev [3,7] **and Tuomas Savolainen** [5,8,9]

[1] Department of Physics, Denison University, Granville, OH 43023, USA
[2] Tuorla Observatory, University of Turku, Väisäläntie 20, 21500 Piikkiö, Finland; talvikki.hovatta@utu.fi
[3] Astro Space Center of Lebedev Physical Institute, Profsoyuznaya 84/32, 117997 Moscow, Russia;
    yyk@asc.rssi.ru (Y.Y.K.); pushkarev.alexander@gmail.com (A.B.P.)
[4] Moscow Institute of Physics and Technology, Dolgoprudny, Institutsky per., 9, 141700 Moscow, Russia
[5] Max-Planck-Institut für Radioastronomie, Auf dem Hügel 69, 53121 Bonn, Germany;
    tuomas.k.savolainen@aalto.fi
[6] Department of Physics and Astronomy, Purdue University, 525 Northwestern Avenue, West Lafayette,
    IN 47907, USA; mlister@purdue.edu
[7] Crimean Astrophysical Observatory, Crimea, 98409 Nauchny, Russia
[8] Aalto University Metsähovi Radio Observatory, Metsähovintie 114, 02540 Kylmälä, Finland
[9] Department of Electronics and Nanoengineering, Aalto University, PL 15500, FI-00076 Aalto, Finland
* Correspondence: homand@denison.edu

Abstract: Combined polarization imaging of radio jets from Active Galactic Nuclei (AGN) in circular and linear polarization, also known as full Stokes imaging, has the potential to constrain both the magnetic field structure and particle properties of jets. Although only a small fraction of the emission when detected, typically less than a few tenths of a percent but up to as much as a couple of percent in the strongest resolved sources, circular polarization directly probes the magnetic field and particles within the jet itself and is not expected to be modified by external screens. A key to using full Stokes observations to constrain jet properties is obtaining a better understanding of the emission of circular polarization, including its variability and spectrum. We discuss what we have learned so far from parsec scale monitoring observations in the MOJAVE program and from multi-frequency observations of selected AGN.

1. Introduction

Polarization observations of jets from Active Galactic Nuclei (AGN) in "full Stokes", combining both linear and circular polarization, have the potential to address fundamental questions about their magnetic field structure and particle populations. Observational constraints on the full three-dimensional magnetic field structure on parsec-scales, near the jet origin in the super-massive black-hole/accretion disk system, are still ambiguous, indicating both that elements of large scale toroidal fields are present (e.g., [1–4]) and that shocks in the jet flow play an important role in the local field order (e.g., [5–7]). Understanding this structure is important to untangling the role magnetic fields may play in continued acceleration and collimation of jets into parsec-scales (e.g., [8,9]). In addition, the low energy end of the relativistic particle spectrum is poorly constrained, yet it can help us understand the particle content and kinetic luminosity of jets (e.g., [10,11]) as well as the particle acceleration mechanisms at work in the jet flow. These low energy particles are potentially observable through their birefringence effects on the polarization, e.g., [12]. One challenge to using

linear polarization alone to answer these questions is that external Faraday screens can significantly modify the observed polarization. Circular polarization, although only a tiny fraction of the jet emission, has the potential to break this degeneracy as it is not expected to be modified by external screens, e.g., [13].

A key step to using full Stokes observations to constrain jet properties is obtaining a better understanding of the emission of circular polarization, including its variability and spectrum. In integrated measurements at ≤ 5 GHz, circular polarization is typically only a small fraction, $\leq 0.1\%$, of the Stokes-I emission [14], with strong values approaching 1% in PKS $2126-158$ [15] and 2–4% in the intra-day variable source PKS $1519-273$ [16]. In VLBA measurements at ≤ 15 GHz, circular polarization is typically $<0.3\%$ with strong values again approaching 1% [17,18] with the strongest observed local value of 3.2% in the jet of 3C 84 [19]. Sources with circular polarization measurements above 0.5% may be more common at higher frequencies [20,21] which probe shorter length-scales in the jet, closer to the central engine. While circular polarization is clearly variable (e.g., [22,23]), there are indications that some sources may show a preferred sign of circular polarization at certain frequencies, e.g., [13,17,22], although this has only been well established for Sgr A* [24,25].

In this proceedings, we first briefly review what is known about the emission mechanisms for circular polarization and discuss the prospects for better constraining the mechanism to answer fundamental questions about jet magnetic fields and particle populations. We then focus on parsec-scale observations from the MOJAVE, Monitoring Of Jets in Active galactic nuclei with VLBA Experiments, program and share preliminary results from multi-epoch measurements of circular polarization in a large number of AGN jets.

2. Emission Mechanisms for Circular Polarization

Circular polarization (CP) can be produced either as an intrinsic component of the emitted synchrotron radiation or through bi-refringence: Faraday conversion of linear polarization into circular, e.g., [26]. Roughly speaking, for optically thin emission, the fraction of intrinsic CP is inversely proportional to the Lorentz factor of the radiating electrons, $m_c \sim 1/\gamma$, and is of order 1% of the Stokes I emission in a uniform magnetic field at centimeter wavelengths [27]. Any field reversals, either along the line of sight or within the telescope beam, will reduce the observed fraction, and of course, if the radiating particles are some mixture of electrons and positrons, the emitted fraction of intrinsic CP will be scaled accordingly. On the other hand, Faraday conversion requires field order in the plane of the sky to convert linear polarization into circular and does not depend on the charge sign of the converting particles. Faraday conversion; however, does require either some magnetic field asymmetry along the line of sight or some internal Faraday rotation of the plane of linear polarization, e.g., [27–29].

In a homogeneous, optically thin region, the spectral dependence of circular polarization is quite different depending on the dominant mechanism. Intrinsic circular polarization is expected to have a shallow spectrum, $m_c \propto \nu^{-0.5}$, while Faraday conversion is expected to be steep, $m_c \propto \nu^{-3}$, if it is due to field asymmetry and perhaps even steeper if the conversion is driven by Faraday rotation which introduces its own frequency dependence [27]. Unfortunately, circular polarization from relativistic synchrotron sources most often coincides with the base of the jet which is expected to be inhomogeneous and have an optical depth near unity. Both emission mechanisms can then have a complex spectrum, including changes of slope and even sign with frequency, making it difficult to discern between them with limited spectral coverage. However, any variations in the field structure, particle density, and optical depth in such a complicated region must affect all Stokes parameters in a consistent way, making it possible to model the full Stokes spectrum to understand not only the emission mechanism but also the physical conditions that give rise to the observed circular polarization.

The first parsec scale results on 3C 279 by [11] favored Faraday conversion as the mechanism, indicating a lower cutoff in the relativistic power-law, particle energy spectrum of $\gamma_l < 20$. Following [10] they argued that a low cutoff in the power-law spectrum implied too large a particle population for an electron-proton jet on kinetic luminosity grounds, indicating that the particle content

of the jet was primarily electron-positron. Subsequent analysis by [12,29] suggested that a contribution by thermal electrons in the jet would relax the relativistic cutoff and permit an electron-proton dominated jet. More detailed, six-frequency spectra obtained by [30] allowed for better modeling of 3C 279, including an inhomogeneous jet base and two homogeneous features close to the jet origin which contribute to the circular and linearly polarized emission. They found that the primary mechanism at higher frequencies was intrinsic circular polarization in the inhomogeneous jet base, suggesting the jet was not in fact e^-e^+ pair dominated. However, emission from the homogeneous components was still best explained by Faraday conversion with a low energy particle cutoff in the range $5 \leq \gamma_l \leq 35$, showing that the two mechanisms may indeed work together in the same source depending on the local conditions. Perhaps the best observations to date constraining the emission mechanism for circular polarization in an AGN jet are the wide-band ATCA observations by [15] of PKS 2126−158. Their detailed, full-Stokes, integrated spectra spanned the full transition from optically thick to optically thin emission and measured a circularly polarized spectra of $m_c \propto \nu^{+0.60 \pm 0.03}$ for the optically thick region and $m_c \propto \nu^{-3.0 \pm 0.4}$ for the optically thin region, matching the expected spectrum for Faraday conversion for the optically thin emission.

3. Circular Polarization from MOJAVE

The MOJAVE program (http://www.physics.purdue.edu/astro/MOJAVE/index.html) [31] monitors the parsec scale structure and evolution of more than 300 AGN jets at 15 GHz with the Very Long Baseline Array (VLBA) in total intensity, linear, and circular polarization. First epoch observations of circular polarization from our original 133 source sample were published in [18], and we found strong circular polarization, $\geq$0.3%, in approximately 15% of our sample. With just a single epoch of observation, we could not detect any trends with source type or degree of linear polarization; however, subsequent analysis by [32] which combined our results with additional observations suggested that Quasars may have stronger circular polarization than BL Lacertae objects on average.

Here we present preliminary multi-epoch results from 2002 through the end of 2009. During this period we observed 278 sources for circular polarization at 15 GHz with an average of six epochs per source. Our methods are nearly the same as those described in our first epoch paper [18] with a couple of differences that are worthy of note. First, all of the results presented here beyond the first published epoch use a final phase calibration assuming no circular polarization to better align the left and right hand phase solutions. As described and tested in [18], this final round of additional phase self-calibration was necessary in some cases due to a clear positive-negative anti-symmetric circular polarization distribution from the gain transfer calibration alone. In that paper, we found that most sources gave very nearly the same results regardless of whether we applied this final round of phase self-calibration assuming zero-V, and on those sources where there was a significant difference, we always preferred the result with the phase self-calibration as more reliable. The second difference worthy of note is that in epochs from 2007 onward, we measure a small, but consistent, offset in circular polarization of order −0.03%. Given its small amplitude, only about one-third of our typical uncertainty of 0.1%, this offset became apparent only after averaging all sources in our 24-h observing runs and examining multiple 24-h experiments. The effect appears to be baseline based, as the offset was not removed by tests that corrected all the antenna gains assuming no source had significant circular polarization. We still do not understand the origin of this offset. It may be due to bandpass or correlator effects that we cannot easily correct; however, given the consistency of the effect and its small size relative to our other uncertainties, we have chosen to simply adjust the measured circular polarization level in all sources in the epochs from 2007 onward by +0.03% and add a 0.03% uncertainty in quadrature with our standard uncertainty values.

Figure 1 shows single epoch linear and circular polarization images of NRAO 140 at 15 GHz along with our multi-epoch measurements of circular polarization from the jet base. Of the 278 sources observed for circular polarization from 2002 through the end of 2009, we found 91 to have at least one

epoch with a three-sigma detection, and 48 sources had multi-epoch three-sigma detections. Typical levels of detected circular polarization range from 0.3 to 0.7% with a few cases up to 1%. NRAO 140, as illustrated in Figure 1, shows consistent circular polarization over epoch, but this behavior is not typical in our sample. It is much more common for detected sources to show variable circular polarization from the jet core, as illustrated in Figure 2.
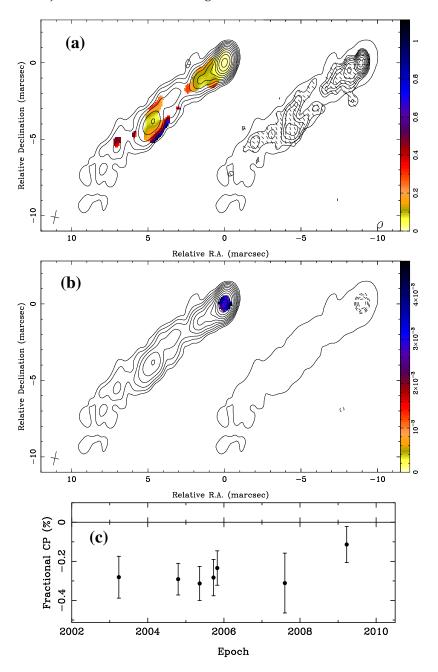

Figure 1. MOJAVE images of the quasar NRAO 140 from 23 September 2005. The left side of panels (**a**,**b**) show total intensity contours over-plotted with fractional linear and circular polarization colorscale respectively. The high levels of linear polarization, exceeding 70% at the extreme jet edge, are an imaging artifact. The right side of the same panels are contours of the linear and circular polarization, with the tick marks in panel (**a**) representing the electric vector position angle. A single total intensity contour is included to show registration. All contour levels in both panels start at 1 mJy/beam and increase in factor of $\sqrt{2}$ steps. The final panel (**c**) shows the fractional circular polarization of the core as a function of epoch.
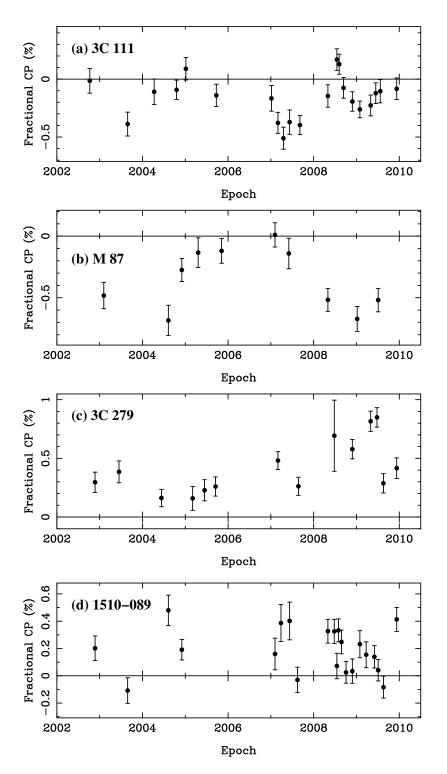
Figure 2. Panels **(a–d)** show fractional circular polarization as a function of epoch in the jet cores of several Active Galactic Nuclei (AGN) with repeated detections of strong circular polarization. As noted in the text, most sources in the our program do not show strong circular polarization, and smaller subset shows repeated detections of strong circular polarization. Of the 39 sources with multi-epoch 3σ detections of circular polarization spanning at least a year, 35 show a preferred sign, as illustrated here.

Sign Consistency

Although variable circular polarization is typical, as illustrated above, it is intriguing that the large majority of our multi-epoch detected sources appear to have a preferred sign of circular polarization.

Repeated detections of the same sign of circular polarization in closely spaced epochs might be expected if there are no rapid changes in opacity during a single outburst, but longer time-scale consistency may be tied to overall magnetic field order in the jet. Several papers have suggested sign consistency at centimeter wavelengths in small numbers of sources or over short intervals [13,17,22] with perhaps the best established case the repeated measurements of Sgr A* over 20 years [24,25]. In our observations reduced to date, we have 39 sources with multi-epoch, three-sigma detections which span at least a year, and 35/39 of those are detected with the same sign as earlier epochs. The median span for those detections is 3.5 years which is longer than a typical outburst at 15 GHz, suggesting that the preferred sign in these sources is set by the super-massive black-hole/accretion disk system, perhaps through a poloidal field component or field helicity [33,34].

It is important to note that sign consistency in a given source may be a function of observing frequency. One of the best studied cases at 15 GHz is 3C 279 which has more than twenty VLBA epochs spanning 14 years (see [17,30] and Figure 2), most of those epochs with strong positive circular polarization and no epochs with negative sign. However, in UMRAO observations at 4.8 GHz, 3C 279 shows repeated changes of sign to negative circular polarization during this time period [30]. Homan et al. [30] argue that these changes in sign are to be expected due to opacity changes during an outburst. Recent results from the POLAMI monitoring program [35] indicate that sources showing a strong sign preference are rarer at 86 GHz, identifying only seven such cases in their 37 source sample. Opacity should not play a major role at this frequency, but it is possible that the smaller length scales probed are dominated by turbulent fields. At 4.8 and 8.4 GHz [36] has recently compared monitoring observations from the F-GAMMA project to those from [22], made more two decades earlier, and find only three sources with stable circular polarization of the same sign in both datasets. Further monitoring is required at a whole range of observing frequencies and time frames to fully establish the degree to which stable magnetic field structures may be important in parsec-scale jets and the time and length scales on which this influence may occur.

References

1. Asada, K.; Inoue, M.; Uchida, Y.; Kameno, S.; Fujisawa, K.; Iguchi, S.; Mutoh, M. A Helical Magnetic Field in the Jet of 3C 273. *Publ. Astron. Soc. Jpn.* **2002**, *54*, L39–L43.
2. Asada, K.; Nakamura, M.; Inoue, M.; Kameno, S.; Nagai, H. Multi-frequency Polarimetry toward S5 0836+710: A Possible Spine-Sheath Structure for the Jet. *Astrophys. J.* **2010**, *720*, 41–45.
3. Gabuzda, D.C.; Murray, É.; Cronin, P. Helical magnetic fields associated with the relativistic jets of four BL Lac objects. *Mon. Not. R. Astron. Soc.* **2004**, *351*, L89–L93.
4. Gabuzda, D.C.; Knuettel, S.; Reardon, B. Transverse Faraday-rotation gradients across the jets of 15 active galactic nuclei. *Mon. Not. R. Astron. Soc.* **2015**, *450*, 2441–2450.
5. Hughes, P.A. The Origin of Complex Behavior of Linearly Polarized Components in Parsec-Scale Jets. *Astrophys. J.* **2005**, *621*, 635–642.
6. Hughes, P.A.; Aller, M.F.; Aller, H.D. Oblique Shocks as the Origin of Radio to Gamma-ray Variability in Active Galactic Nuclei. *Astrophys. J.* **2011**, *735*, 81.

7.   Marscher, A.P. Turbulent, Extreme Multi-zone Model for Simulating Flux and Polarization Variability in Blazars. *Astrophys. J.* **2014**, *780*, 87.

8.   Vlahakis, N.; Königl, A. Magnetic Driving of Relativistic Outflows in Active Galactic Nuclei. I. Interpretation of Parsec-Scale Accelerations. *Astrophys. J.* **2004**, *605*, 656–661.

9.   Komissarov, S.S.; Barkov, M.V.; Vlahakis, N.; Königl, A. Magnetic acceleration of relativistic active galactic nucleus jets. *Mon. Not. R. Astron. Soc.* **2007**, *380*, 51–70.

10. Celotti, A.; Fabian, A.C. The Kinetic Power and Luminosity of Parsecscale Radio Jets—An Argument for Heavy Jets. *Mon. Not. R. Astron. Soc.* **1993**, *264*, 228–236.

11. Wardle, J.F.C.; Homan, D.C.; Ojha, R.; Roberts, D.H. Electron-positron jets associated with the quasar 3C 279. *Nature* **1998**, *395*, 457–461.

12. Beckert, T.; Falcke, H. Circular polarization of radio emission from relativistic jets. *Astron. Astrophys.* **2002**, *388*, 1106–1119.

13. Homan, D.C.; Attridge, J.M.; Wardle, J.F.C. Parsec-Scale Circular Polarization Observations of 40 Blazars. *Astrophys. J.* **2001**, *556*, 113–120.

14. Weiler, K.W.; de Pater, I. A catalog of high accuracy circular polarization measurements. *Astrophys. J. Suppl.* **1983**, *52*, 293–327.

15. O'Sullivan, S.P.; McClure-Griffiths, N.M.; Feain, I.J.; Gaensler, B.M.; Sault, R.J. Broad-band radio circular polarization spectrum of the relativistic jet in PKS B2126-158. *Mon. Not. R. Astron. Soc.* **2013**, *435*, 311–319.

16. Macquart, J.P.; Kedziora-Chudczer, L.; Rayner, D.P.; Jauncey, D.L. Strong, Variable Circular Polarization in PKS 1519-273. *Astrophys. J.* **2000**, *538*, 623–627.

17. Homan, D.C.; Wardle, J.F.C. Detection and Measurement of Parsec-Scale Circular Polarization in Four AGNS. *Astron. J.* **1999**, *118*, 1942–1962.

18. Homan, D.C.; Lister, M.L. MOJAVE: Monitoring of Jets in Active Galactic Nuclei with VLBA Experiments. II. First-Epoch 15 GHz Circular Polarization Results. *Astron. J.* **2006**, *131*, 1262–1279.

19. Homan, D.C.; Wardle, J.F.C. High Levels of Circularly Polarized Emission from the Radio Jet in NGC 1275 (3C 84). *Astrophys. J. Lett.* **2004**, *602*, L13–L16.

20. Vitrishchak, V.M.; Gabuzda, D.C.; Algaba, J.C.; Rastorgueva, E.A.; O'Sullivan, S.P.; O'Dowd, A. The 15–43 GHz parsec-scale circular polarization of 41 active galactic nuclei. *Mon. Not. R. Astron. Soc.* **2008**, *391*, 124–135.

21. Agudo, I.; Thum, C.; Gómez, J.L.; Wiesemeyer, H. A simultaneous 3.5 and 1.3 mm polarimetric survey of active galactic nuclei in the northern sky. *Astron. Astrophys.* **2014**, *566*, A59.

22. Komesaroff, M.M.; Roberts, J.A.; Milne, D.K.; Rayner, P.T.; Cooke, D.J. Circular and linear polarization variations of compact radio sources. *Mon. Not. R. Astron. Soc.* **1984**, *208*, 409–425.

23. Aller, H.D.; Aller, M.F.; Plotkin, R.M. Circular Polarization Variability in Extragalactic Sources on Time Scales of Months to Decades. *Astrophys. Space Sci.* **2003**, *288*, 17–28.

24. Bower, G.C.; Falcke, H.; Sault, R.J.; Backer, D.C. The Spectrum and Variability of Circular Polarization in Sagittarius A* from 1.4 to 15 GHz. *Astrophys. J.* **2002**, *571*, 843–855.

25. Muñoz, D.J.; Marrone, D.P.; Moran, J.M.; Rao, R. The Circular Polarization of Sagittarius A* at Submillimeter Wavelengths. *Astrophys. J.* **2012**, *745*, 115.

26. Jones, T.W.; Odell, S.L. Transfer of polarized radiation in self-absorbed synchrotron sources. I—Results for a homogeneous source. *Astrophys. J.* **1977**, *214*, 522–539.

27. Wardle, J.F.C.; Homan, D.C. Theoretical Models for Producing Circularly Polarized Radiation in Extragalactic Radio Sources. *Astrophys. Space Sci.* **2003**, *288*, 143–153.

28. Jones, T.W. Polarization as a probe of magnetic field and plasma properties of compact radio sources— Simulation of relativistic jets. *Astrophys. J.* **1988**, *332*, 678–695.

29. Ruszkowski, M.; Begelman, M.C. Circular Polarization from Stochastic Synchrotron Sources. *Astrophys. J.* **2002**, *573*, 485–495.

30. Homan, D.C.; Lister, M.L.; Aller, H.D.; Aller, M.F.; Wardle, J.F.C. Full Polarization Spectra of 3C 279. *Astrophys. J.* **2009**, *696*, 328–347.

31. Lister, M.L.; Aller, H.D.; Aller, M.F.; Cohen, M.H.; Homan, D.C.; Kadler, M.; Kellermann, K.I.; Kovalev, Y.Y.; Ros, E.; Savolainen, T.; et al. MOJAVE: Monitoring of Jets in Active Galactic Nuclei with VLBA Experiments. V. Multi-Epoch VLBA Images. *Astron. J.* **2009**, *137*, 3718–3729.

32. Vitrishchak, V.M.; Pashchenko, I.N.; Gabuzda, D.C. Circular polarization—Another difference between quasars and BL Lac objects? *Astron. Rep.* **2010**, *54*, 269–276.

33. Hodge, P.E. Circular polarization from compact extragalactic radio sources as a result of nonuniform magnetic fields. *Astrophys. J.* **1982**, *263*, 595–598.

34. Enßlin, T.A. Does circular polarisation reveal the rotation of quasar engines? *Astron. Astrophys.* **2003**, *401*, 499–504.

35. Thum, C.; Agudo, I.; Molina, S.N.; Casadio, C.; Gómez, J.L.; Morris, D.; Ramakrishnan, V.; Sievers, A. POLAMI: Polarimetric Monitoring of Active Galactic Nuclei at Millimetre Wavelengths—II. Widespread circular polarization. *Mon. Not. R. Astron. Soc.* **2018**, *473*, 2506–2520.

36. Myserlis, I.; Angelakis, E.; Kraus, A.; Liontas, C.A.; Marchili, N.; Aller, M.F.; Aller, H.D.; Karamanavis, V.; Fuhrmann, L.; Krichbaum, T.P.; et al. Full-Stokes polarimetry with circularly polarized feeds—Sources with stable linear and circular polarization in the GHz regime. *ArXiv* **2017**, arXiv:astro-ph.IM/1706.04200.